Particle-tracking simulations of anomalous transport in hierarchically fractured rocks

Delphine Roubinet [a,*], Jean-Raynald de Dreuzy [b], Daniel M. Tartakovsky [a]

[a] Department of Mechanical and Aerospace Engineering, University of California, San Diego, 9500 Gilman Dr., La Jolla, CA 92093, USA
[b] Géosciences Rennes, UMR CNRS 6118, Université de Rennes I, Rennes, France

ARTICLE INFO

ABSTRACT

Complex topology of fracture networks and interactions between transport processes in a fracture and the ambient un-fractured rock (matrix) combine to render modeling solute transport in fractured media a challenge. Classical approaches rely on both strong assumptions of either limited or full diffusion of solutes in the matrix and simplified fracture configurations. We analyze fracture-matrix transport in two-dimensional Sierpinski lattice structures, which display a wide range of matrix block sizes. The analysis is conducted in several transport regimes that are limited by either diffusion or block sizes. Our simulation results can be used to validate the simplifying assumptions that underpin classical analytical solutions and to benchmark other numerical methods. They also demonstrate that both hydraulic and structural properties of fractured rocks control the residence time distribution.

© 2012 Elsevier Ltd. All rights reserved.

1. Introduction

Solute transport in fractured porous media often exhibits anomalous (non-Fickian) characteristics that, if ignored, can compromise both site characterization and model reliability (Berkowitz, 2002; Carrera et al., 1998; Neuman, 2005; Zhou et al., 2007). Spatial and/or statistical heterogeneity of fracture networks and interactions between transport processes in a fracture and the ambient un-fractured rock (matrix) are two mechanisms that are responsible for this non-Fickian behavior. The former affects hydraulic properties of fractured rocks (Bonnet et al., 2001; Bour and Davy, 1999; Davy et al., 2006, 2010; de Dreuzy et al., 2001; Doughty and Karasaki, 2002), while the latter controls long-term transport characteristics (Birgersson and Neretnieks, 1990; Dershowitz and Miller, 1995; Haggerty et al., 2000; Neretnieks, 1980). Solutes are delayed by exchange between the high-velocity fracture paths and the poorly permeable matrix as well as by solute adsorption within the matrix. Fracture-matrix exchange is driven by (1) solute dynamics within the fractures conditioning the transfer to the matrix blocks (Carrera et al., 1998; Hamm and Bidaux, 1996; Hassanzadeh and Pooladi-Darvish, 2006), (2) geometrical structures of the blocks (Crank, 1975; Dershowitz and Miller, 1995; Warren and Root, 1963) and (3) heterogeneity of transfer processes and porosity (Bai et al., 1993; Haggerty and Gorelick, 1995; Lagendijk et al., 2000).

While both the network structure and natural (or experimental) physical conditions affect fracture-matrix exchange and thus the residence time distribution, classical models generally focus on just one of these two mechanisms and ignore (or strongly simplify) the other. On the one hand, the dual-porosity approach assumes that fractures and ambient matrix can be independently homogenized and that exchange between them depends on a single coefficient (Barenblatt and Zheltov, 1960; Warren and Root, 1963). On the other hand, the single fracture approach reduces fracture networks to a single fracture or a set of parallel fractures embedded in a homogeneous matrix (Sudicky and Frind, 1982; Tang et al., 1981). These approaches employ simplified models of diffusion in matrix blocks, ignoring (or simplifying) the effects of block shapes and sizes, and fracture hydraulics. More recent modeling frameworks employ shape factors (Hassanzadeh et al., 2009; Lim and Aziz, 1995), multi-rate mass transfer (Haggerty and Gorelick, 1995) or memory functions (Carrera et al., 1998) to account for the fracture-matrix exchange in more realistic settings. Yet their reported applications are mostly limited to idealized systems, such as layered, cylindrical or spherical exchange. Roubinet et al. (2010) proposed a particle-tracking algorithm that is especially adapted to heterogeneous fractured porous media with multiple matrix block sizes.

We deploy the Roubinet et al. (2010) algorithm (code PERFORM) to simulate solute migration in fracture networks exhibiting an evolving range of matrix block distribution, in several transport regimes. Our analysis aims to (1) establish benchmark solutions of solute transport in complex fractured media characterized by a

---

* Corresponding author. Tel.: +1 858 822 3031.
E-mail address: delphine.roubinet@gmail.com (D. Roubinet).

distribution of matrix bock sizes, (2) evaluate the validity of classical modeling concepts, and (3) identify characteristic diffusion regimes of solute transport in complex fractured media. Section 2 contains a formulation of benchmark problems, and the numerical algorithm for solving these problems is described in Section 3. The resulting breakthrough curves are presented in Section 4, and used in Section 5 to identify various diffusion regimes.

2. Formulation of benchmark problems

The Sierpinski lattices are hierarchical fractal structures that exhibit high degrees of connectivity imposed by a set of continuous elements (Doughty and Karasaki, 2002). Several studies have demonstrated that the high degree of connectivity of these structures provides an adequate representation of the heterogeneity of natural fractured media (Davy et al., 2006; de Dreuzy and Davy, 2007; Doughty and Karasaki, 2002; Sahimi, 1993). The Sierpinski lattices are generated by recursively shrinking and replicating a pattern through scales. Structures are controlled by a density parameter directly linked to the fractal dimension of the resulting structure (de Dreuzy and Davy, 2007) and the level of recursive divisions k. We are mostly interested in the extent of the block-scale distribution parameterized by k and consider three structures with $k=1$, 2, or 3 (Fig. 1).

The basis configuration ($k=1$) corresponds to a regular fracture network, which is used as a reference. Increasing the magnitude of k ($k=2$ and $k=3$) increases structure heterogeneity. In what follows, we refer to the three block geometries generated by the case $k=3$ in Fig. 1 as large, medium and small blocks.

Unless specified otherwise, simulations are conducted with the following parameters: the domain length is set to $L=100$ m, the fracture aperture to $2b=10^{-4}$ m, the matrix porosity to $\phi_m=0.1$, and the matrix diffusion coefficient to $D_m=10^{-8}$ m²/s (corresponding to molecular diffusion coefficient multiplied by a tortuosity factor). Periodic boundary conditions and a uniform head gradient (∇h) are applied in the vertical and horizontal directions respectively. Simulations are conducted for several values of the head gradient corresponding to the fracture flow velocity $v=10^{-1}$ m/s (Fast Flows), 10^{-3} m/s (Medium Flows) and 10^{-4} m/s (Slow Flows) for the simplest configuration (Fig. 1, $k=1$). These velocities have been selected to identify characteristic regimes and their extension for the range of velocities typically used for field tracer tests, i.e., 10^{-2}–10^{-6} m/s (Zhou et al., 2007).

Solute transport is analyzed through the residence time distribution within the domain. Particles are injected at the inlet (left side of the domain) within the fractures and their residence time is recorded at the domain outlet. The residence-time distributions

from 10.000 particles are similar to those obtained from 100.000 particles and are presented in Section 4.

3. Simulation algorithm

Classical solute transport models rely on simplified network structures and/or diffusion regimes. To simulate solute transport on a large range of structural and hydraulic properties, we use the particle-tracking approach of Roubinet et al. (2010) that is specifically designed for highly heterogeneous fractured porous media. This modeling method enables one to handle (1) heterogeneous hydraulic properties of fracture networks, (2) unlimited or limited diffusion within matrix blocks, and (3) a wide distribution of matrix block sizes.

For a particle advecting during the time t_a in the fracture, its diffusion time t_{diff} in the surrounding infinite matrix is estimated by (Painter and Cvetkovic, 2005)

$$t_{diff} = \left(\frac{\phi_m \sqrt{D_m}}{2\alpha b} t_a \right)^2 \tag{1}$$

where ϕ_m and D_m are the matrix porosity and diffusion coefficient respectively, b is the fracture half-aperture, and $\alpha = \mathrm{erfc}^{-1}(U[0,1])$ with $U[0,1]$ denoting a uniform random number in the interval $[0,1]$. The corresponding penetration depth x_{diff} into the matrix is

$$x_{diff} = \frac{\phi_m D_m}{\sqrt{2} \alpha b v} l \tag{2}$$

where l is the length of the fracture segment and v is the fracture flow velocity. We define a fracture segment as the segment delimited by two fracture intersection points.

The assumption of infinite matrix corresponds to a diffusive regime not limited by structural properties. Expressions (1) and (2) remain valid as long as particles do not reach one of the neighboring fractures by diffusion through the matrix blocks. This condition can be expressed as $x_{diff} < B$, where B is the distance from the initial fracture to the closest neighboring fractures. For the specific square matrix blocks configuration in Fig. 1, the closest neighboring fracture of a fracture segment of length l is located at the same distance $B=l$. Solute diffusion is thus not limited by structural properties for small values of the characteristic ratio β_1 expressed as

$$\beta_1 = \frac{\phi_m D_m}{b v} \tag{3}$$

and corresponding to a modified inverted Péclet number where the characteristic length is the fracture aperture instead of the fracture length.

For larger values of the characteristic ratio β_1, diffusion may be limited by the size of the block, and particles may transfer to a neighboring fracture through the matrix block one (or several) time(s). The required characteristic diffusion time t_B to cross the

Sierpinski lattice structures			
Division level	$k=1$	$k=2$	$k=3$
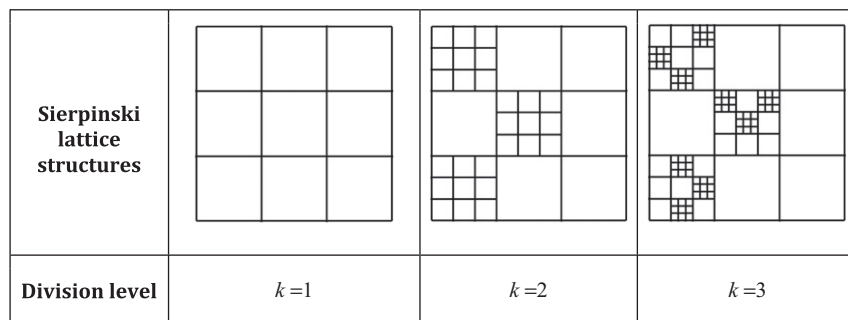
Fig. 1. The Sierpinski lattices with evolving ranges of the block size distribution for domain size $L=100$ m and fracture aperture $2b=10^{-4}$ m.

matrix block of size B is given by

$$t_B = \frac{B^2}{2D_m}. \tag{4}$$

The total diffusion time spent in the block is

$$t_{diff} = Nt_B \tag{5}$$

and the number of times that the particle diffuses through the matrix block, N, is expressed as

$$N = \frac{t_a}{t_a^*} \tag{6}$$

where t_a^* corresponds to the required residence time within the fracture to diffuse during the time t_B in the matrix blocks. From expression (1) the characteristic times t_a^* and t_B are related as

$$t_a^* \propto \frac{b}{\phi_m \sqrt{D_m}} \sqrt{t_B}. \tag{7}$$

Combining the latter expression with expressions (4) and (6), the total diffusion in a block, expressed by expression (5), is related to the advection along this block by

$$t_{diff} \propto \frac{\phi_m B}{b} t_a. \tag{8}$$

Expressions (1) and (8) characterize diffusion time in matrix blocks for diffusion regime unlimited and limited by structural properties respectively. For the first regime, diffusion and advection times are quadratically related to the ratio $\gamma_1 = \phi_m \sqrt{D_m}/b$ independent of structural properties (parameter B). For the second regime, diffusion and advection times are linearly related to the ratio $\gamma_2 = \phi_m B/b$ that does not depend on the matrix diffusion coefficient (parameters D_m) as demonstrated by Carrera et al. (1998).

These key concepts allow one to consider the impact of fracture properties (and thus hydraulic properties) in both diffusion regimes, and the impact of structural properties (e.g. block size) in the full diffusion regime. This is in contrast to the classical models that are usually restricted to a predetermined diffusion regime, wherein diffusion times are driven by either hydraulic or structural properties.

It is worth emphasizing that the presented modeling approach assumes one-dimensional diffusion in matrix blocks. This classical assumption for modeling solute transport in fractured porous media is valid for the configurations and conditions of the current study (Roubinet et al., 2012). Finally, the matrix mesh-free property of the method limits simulation times to several minutes and 1 h for 10.000 and 100.000 particles respectively. Fracture network discretization is characterized by the limiting transfer probability p_{lim} defined by expression (8) of Roubinet et al. (2010) and set to 0.1.

4. Residence-time distribution for Sierpinski lattice structures

Fig. 2a–d shows cumulative arrival times computed with the algorithm described above. The black circles, blue squares and green triangles represent the arrival times for the Sierpinski lattices with $k=1$, 2, and 3 levels of divisions respectively. Fig. 2a–c correspond respectively to the *Fast*, *Medium* and *Slow Flows* (see Section 2). Fig. 2d shows the cumulative arrival times for the *Slow Flows* 2 configuration, whose parameters are identical to those of the *Slow Flows* regime except for the matrix diffusion coefficient $D_m = 10^{-6}$ m²/s. (The latter value of D_m characterizes a dual-porosity medium in which the matrix represents both a safe rock and small fractures that are not explicitly represented by a fracture network due to either prohibitive computational costs or the lack of sufficient data.)

For *Fast Flows* (Fig. 2a), the division level of the lattice influences the breakthrough-curve position as the median arrival time increases about half-order of magnitude with the level of division k. This influence decreases by decreasing the flow velocity v in the fracture network as arrival times of the complex cases ($k=2$ and $k=3$) tend to the ones of the basis case ($k=1$). The convergence is observed first for long arrival times (*Medium Flows* experience, Fig. 2b) and then for short arrival times (*Slow Flows* 1 experience, Fig. 2c). It leads to reduce the arrival time range of the complex cases resulting in similar curves for both basis and complex cases (Fig. 2c). Breakthrough curves from the two kinds of configurations (basis and complex) are again distinguishable by increasing the matrix diffusion coefficient D_m (*Slow Flows* 2 experience, Fig. 2d). Whereas curve position remains similar, a strong reduction of the arrival time range is observed for the basis case (from Fig. 2c to d).

It must be noticed that decreasing velocity about two orders of magnitude results in a median arrival time around four orders of magnitude larger for the basis configuration (from Fig. 2a to b). For the complex cases, the long arrival times converge by decreasing the flow velocity about two orders of magnitude (Fig. 2b) whereas the short ones converge by decreasing it about one order more (Fig. 2c).

From the previous observations, the hierarchical organization of the studied structures impacts arrival time distribution properties. It influences arrival time amplitude (characterized by the median arrival time) when advection is the dominant process (*Fast Flows* case) whereas it influences their range (characterized by the variance) when diffusion is the dominant process (*Slow Flows* 2 case). Results for intermediary configurations (*Medium Flows* and *Slow Flows* 1 cases) must be a combination of the two previous extreme behaviors.

5. Characteristic regimes and alternative modeling concepts

The residence time distributions reported in the previous section are compared to two classical approaches adapted either to small matrix diffusion compared to fracture advection (assumption of infinite matrix) (Cvetkovic et al., 2004; Maloszewski and Zuber, 1993; Tang et al., 1981) or to regular parallel fracture networks where diffusion may be limited by the fracture spacing (Liu et al., 2000; Shan and Pruess, 2005; Sudicky and Frind, 1982). We denote these two models as *Hydraulic Sierpinski* and *Regular Layers* respectively and results presented in the previous section are denoted *Full Sierpinski*. The objectives are both to assess the relevance of classical models in this benchmark context and second to identify and characterize the different transport regimes. We organize the comparison around the three fast, medium and slow flow cases.

5.1. Solute behavior for fast flows

Fig. 3a shows the good agreement between the *Full Sierpinski* (large full symbols) and the *Hydraulic Sierpinski* (small empty symbols) approaches for the *Fast Flows* experience. It means that the diffusive penetration depth in the matrix is too small to allow particle transfer through the matrix block by diffusing from the initial fracture to one of the neighboring fractures. In other words, the assumption of infinite matrix related to the *Hydraulic Sierpinski* approach is valid and diffusion regime is not impacted by the structural properties.

Residence time distribution does not depend on the block size distribution but solely on the fracture velocity and aperture distributions and on the matrix diffusion. Such regime will remain for smaller values of the dimensionless parameter β_1, with $\beta_1 = 10^{-4}$ in this present case.
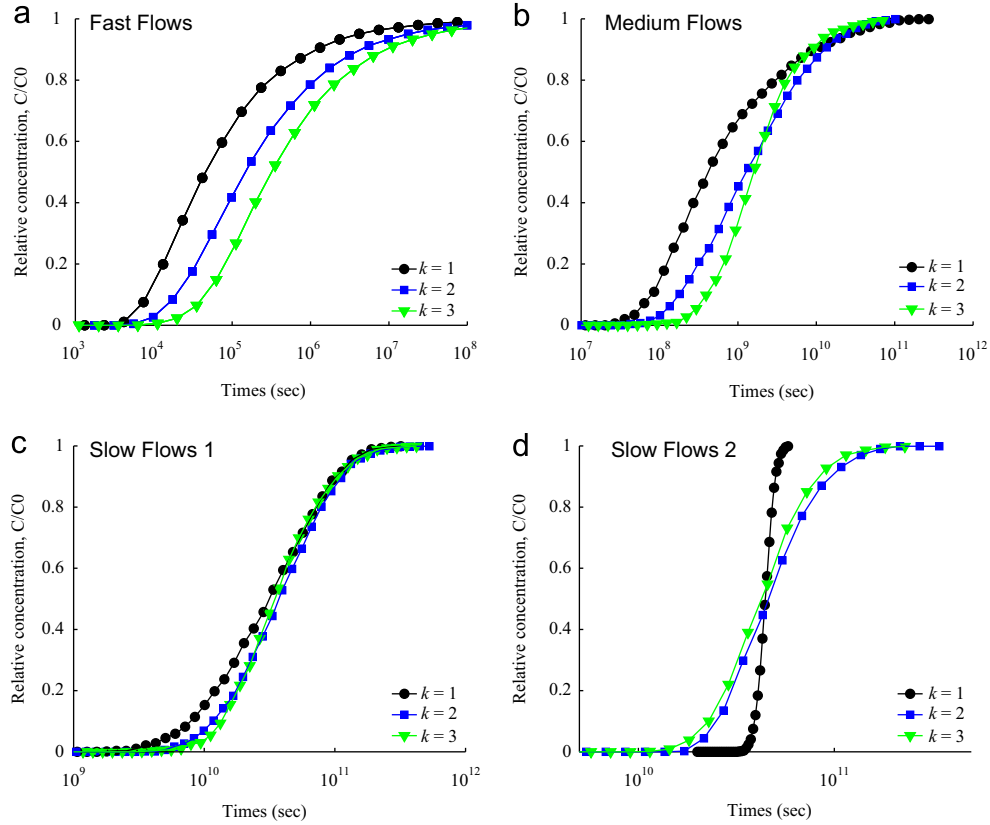
Fig. 2. Breakthrough curves for the generated Sierpinski lattice structures (Fig. 1) where k represents the level of division. Black circles, blue squares and green triangles are the results for one, two and three level(s) of division respectively. Results are obtained for the sets of parameters described in Section 2 and *Slow Flows* 1 and *Slow Flows* 2 correspond to the *Slow Flows* configuration with the matrix diffusion coefficient D_m set to 10^{-8} m²/s and 10^{-6} m²/s respectively. (For interpretation of the references to color in this figure caption, the reader is referred to the web version of this article.)
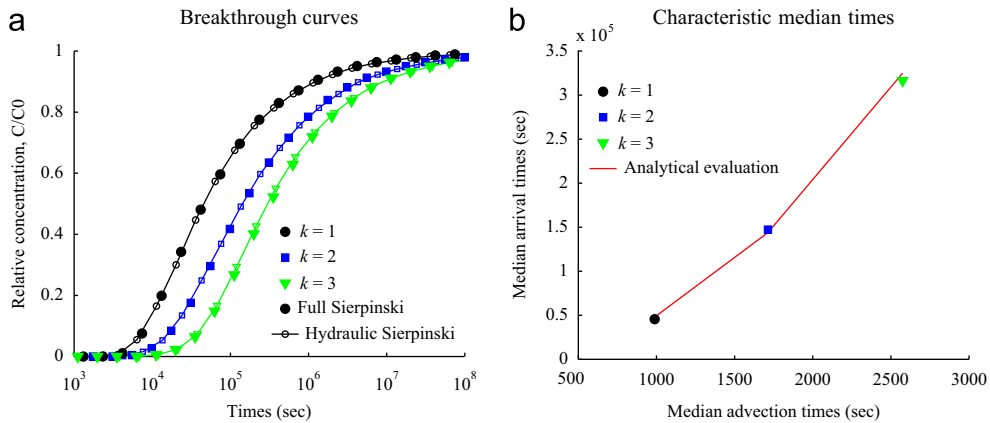
Fig. 3. (a) Breakthrough curves for the generated Sierpinski lattice structures (Fig. 1) and for the set of parameters denoted *Fast Flows* (Section 2). Black circles, blue squares and green triangles represent arrival times for $k=1$, $k=2$ and $k=3$ respectively. Large full symbols and small empty symbols are the simulation results from the *Full Sierpinski* and *Hydraulic Sierpinski* approaches respectively. (b) Symbols and the red line represent the relation between median advection times and median arrival times from numerical results (*Full Sierpinski* approach) and the analytical expression (9) respectively. (For interpretation of the references to color in this figure caption, the reader is referred to the web version of this article.)

For the present regime, diffusion times in matrix blocks are related to advection times in fractures by the expression (1). As expected, it implies a non-linear dependence between the arrival times (T_{arr}) and the total advection times in the fracture network (T_a) as the red line of Fig. 3b is obtained for the expression

$$T_{arr} = \gamma_1 T_a^2 \qquad (9)$$

where $\gamma_1 = \phi_m \sqrt{D_m}/b$.

It must be noticed that the advection time increase from a configuration to another is due to longer paths and to smaller velocities within the smaller fractures.

5.2. Solute behavior for medium flows

Fig. 4 shows solute behavior for the set of parameters denoted *Medium Flows* that corresponds to a larger value of the previously defined characteristic ratio β_1 ($\beta_1 = 10^{-2}$). As previously, large full and small empty symbols represent simulation results from *Full Sierpinski* and *Hydraulic Sierpinski* approaches respectively and red full, dashed and dotted lines represent simulation results for *Regular Layers 1*, *Regular Layers 2* and *Regular Layers 3* configurations respectively. These three latter approaches correspond to parallel fracture networks spaced out by the largest, intermediate
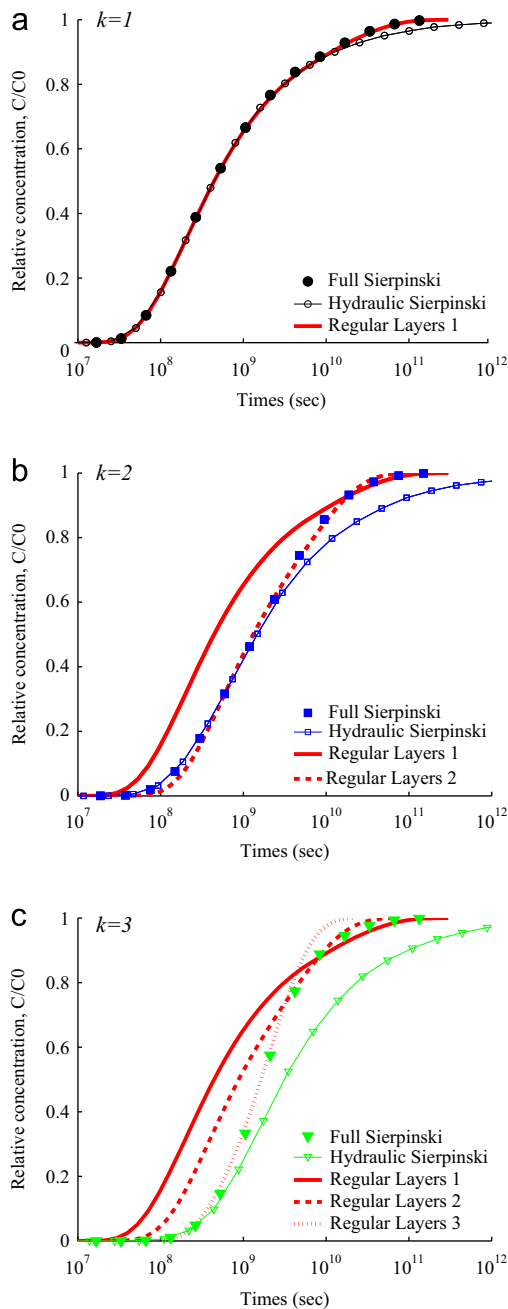
Fig. 4. Breakthrough curves for the generated Sierpinski lattice structures (Fig. 1) with a level of division (a) $k=1$, (b) $k=2$ and (c) $k=3$. Large full and small empty symbols represent simulation results from the *Full Sierpinski* and *Hydraulic Sierpinski* approaches respectively. Red full, dashed and dotted lines are simulation results from the *Regular Layers 1*, *Regular Layers 2* and *Regular Layers 3* approaches respectively. (For interpretation of the references to color in this figure caption, the reader is referred to the web version of this article.)

and smallest block observed on the generated Sierpinski lattice structures respectively (Fig. 1).

Increasing flow velocity from the previous simulations (*Fast Flows*) leads to an intermediate regime where both hydraulic and structural properties impact solute behavior. Arrival times are first driven by hydraulic properties (where results from *Full Sierpinski* and *Hydraulic Sierpinski* approaches are similar) and then driven by structural properties (where results from *Full Sierpinski* and *Regular Layers* approaches are similar). In this latter regime, diffusion is progressively limited by the several block sizes from the smallest one to the largest one for each configuration.

Considering that diffusion times in matrix blocks characterize arrival times, transition times between the several observed regimes can be evaluated by the expression (4) corresponding to the first times where diffusion is limited by blocks of size B. For the present study, solute behavior for the simplest configuration ($k=1$) is characterized by two regimes and $t_{b=33.3}$ represents the transition time between the first regime (where hydraulic properties are determinant) and the second regime (where diffusion is limited by large blocks) (Fig. 4a). The second configuration ($k=2$) is characterized by three regimes where solute behavior is driven first by hydraulic properties, secondly by the medium blocks and then by the large blocks and the corresponding transition times are $t_{b=11.1}$ and $t_{b=33.3}$ respectively (Fig. 4b). And finally the last configuration ($k=3$) presents four regimes characterized first by hydraulic properties and then by the several kinds of blocks from the smallest one to the largest one. The corresponding transition times are $t_{b=3.7}$, $t_{b=11.1}$ and $t_{b=33.3}$.

5.3. Solute behavior for slow flows

Figs. 5 and 6 show simulation results for the set of parameters denoted *Slow Flows* 1 ($\beta_1 = 10^{-1}$) and *Slow Flows* 2 ($\beta_1 = 10$) respectively. Contrary to the previous case (*Medium Flows*), influence of hydraulic properties is poorly visible as simulation results from the *Hydraulic Sierpinski* approach overestimate arrival times on the main parts of the curves (Fig. 5a). The characteristic ratio β_1 is large enough to offer a configuration where diffusion regime is mainly limited by structural properties. For the complex cases, arrival times are influenced first by the smallest block size and then by the largest one (Fig. 5b).

For the largest value of β_1 (*Slow Flows* 2), the range of arrival times is strongly reduced for the simple case showing that diffusion into matrix blocks is instantaneously limited by structural properties (Fig. 6a). For complex cases, the actual range of arrival times is due to the standard deviation of advection times as shown by Fig. 6b. The red line is obtained for the relation

$$\sigma(T_{arr}) = \gamma_2 \sigma(T_a) \tag{10}$$

where $\sigma(T)$ is the standard deviation of the times T, T_{arr} and T_a are the arrival times and the total advection times in the fracture network and $\gamma_2 = \phi_m B/b$ with B the size of the largest block. This is coherent with expression (8) related diffusion and advection times for large values of the ratio β_1 and shows that structural properties impact the amplitude of arrival times whereas hydraulic properties impact their range of variation.

6. Conclusions

The present work demonstrates key results for the understanding of solute behavior in heterogeneous fractured porous media. It shows that the characteristic ratio enables one to identify diffusion regimes occurring in the domain and thus to determine the key properties impacting arrival times and the appropriate modeling approaches.

- For small values of the ratio β_1, solute behavior is driven by the hydraulic properties of the medium and thus by the heterogeneity level of the fracture network. Classical models neglecting the effect of structural properties (assumption of infinite matrix) and focusing on the fracture network properties (Discrete Fracture Network representation) are particularly relevant.
- For large values of the ratio β_1, solute behavior is driven by both structural and hydraulic properties as they determine the amplitude and variance of arrival times respectively. Structural properties can be simplified as their impact is mainly
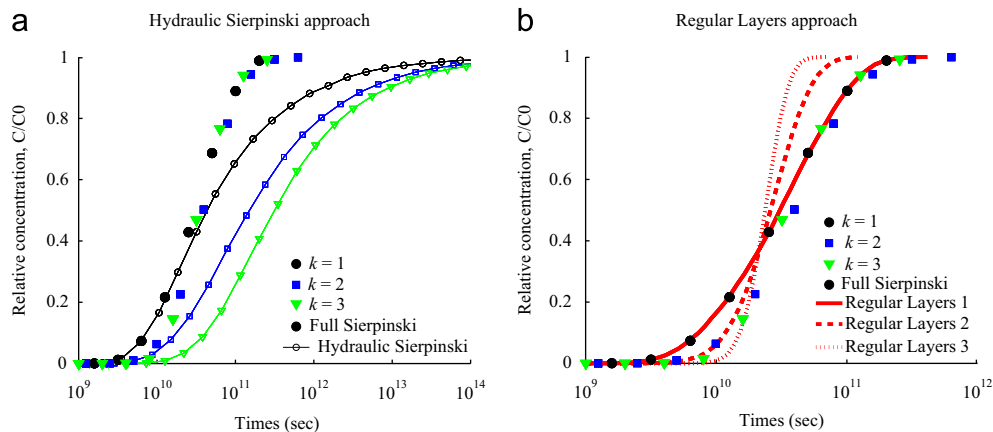
Fig. 5. Simulation results from the *Full Sierpinski* approach (full large symbols) are compared to simulation results from (a) the *Hydraulic Sierpinski* and (b) the *Regular Layers* approaches. Black circles, blue squares and green triangles represent arrival times for the generated Sierpinski lattice structures (Fig. 1) with $k=1$, $k=2$ and $k=3$ respectively. Red large lines are simulation results from the *Regular Layers* approaches with a fracture spacing corresponding to the largest, the medium and the smallest blocks size for the full, dashed and dotted lines respectively. (For interpretation of the references to color in this figure caption, the reader is referred to the web version of this article.)
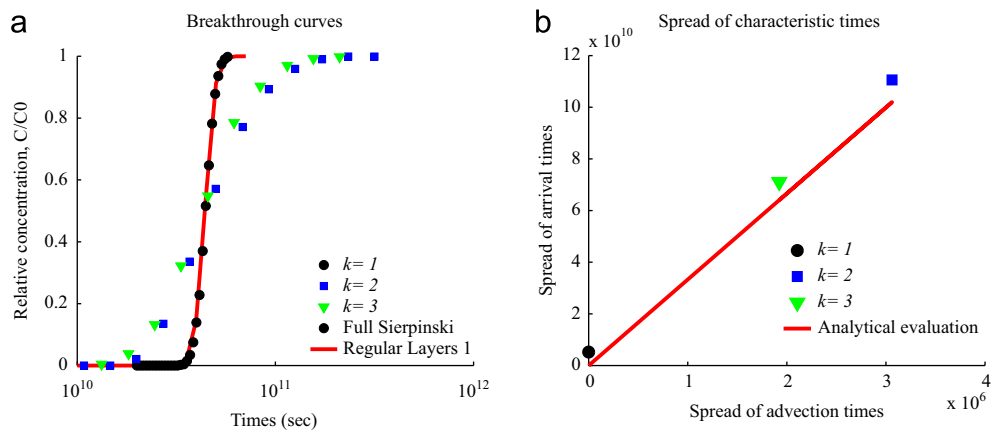
Fig. 6. (a) Breakthrough curves for the generated Sierpinski lattice structures (Fig. 1) and for the set of parameters denoted *Slow Flows* 2. Black circles, blue squares and green triangles represent arrival times for $k=1$, $k=2$ and $k=3$ respectively. Large full symbols and the red line are simulation results from the *Full Sierpinski* and the *Regular Layer 1* approach respectively. (b) Symbols and the red line represent the relation between spreads of advection and arrival times from numerical results (*Full Sierpinski* approach) and the analytical expression (10) respectively. (For interpretation of the references to color in this figure caption, the reader is referred to the web version of this article.)

related to the largest block of the structure. A simple parallel fracture network representation is thus able to approximate median arrival times but not the range of the arrival time distribution.

- For intermediary values of β_1, first arrival times are driven by hydraulic properties whereas the following ones are driven by the block size distribution, with a progressive influence from the smallest to largest block of the domain. This regime requires sophisticated modeling approaches enable to consider both hydraulic and structural properties.

The presented results and their interpretation are formulated in terms relevant to contaminant transport in fractured porous media. However, this study and the underlying methodology are directly applicable to many phenomena in petroleum and geothermal engineering, which both exhibit complex interactions between transport mechanisms and take place in fractured media with heterogeneous structures. By extending the modeling approach, future benchmarks could consider reactive transport, 3D media and the full dimensionality of matrix diffusion. The two latter extensions are particularly pertinent for oil extraction and heat transport where the volume of matrix blocks and its investigation are determinant factors for the performance of the system.

Acknowledgement

References

Bai, M., Elsworth, D., Roegiers, J.C., 1993. Multiporosity multipermeability approach to the simulation of naturally fractured reservoirs. Water Resources Research 29, 1621–1633. (PT: J; TC: 53; UT: WOS:A1993LE49500011).

Barenblatt, G.I., Zheltov, I.P., 1960. Fundamental equations for the filtration of homogeneous fluids through fissured rocks. Doklady Akademii Nauk SSSR 132, 545–548. (PT: J; TC: 56).

Berkowitz, B., 2002. Characterizing flow and transport in fractured geological media: a review. Advances in Water Resources 25, 861–884. (PT: J; TC: 167).

Birgersson, L., Neretnieks, I., 1990. Diffusion in the matrix of granitic rock—field-test in the stripa mine. Water Resources Research 26, 2833–2842. (PT: J; TC: 31; UT: WOS:A1990EH66800020).

Bonnet, E., Bour, O., Odling, N., Davy, P., Main, I., Cowie, P., Berkowitz, B., 2001. Scaling of fracture systems in geological media. Reviews of Geophysics 39, 347–383. (PT: J; NR: 210; TC: 230; J9: REV GEOPHYS; PG: 37; GA: 458WM).

Bour, O., Davy, P., 1999. Clustering and size distributions of fault patterns: theory and measurements. Geophysical Research Letters 26, 2001–2004. (PT: J; NR: 18; TC: 41; J9: GEOPHYS RES LETT; PG: 4; GA: 213TU).

Carrera, J., Sanchez-Vila, X., Benet, I., Medina, A., Galarza, G., Guimera, J., 1998. On matrix diffusion: formulations, solution methods and qualitative effects. Hydrogeology Journal 6, 178–190. (PT: J; TC: 86).

Crank, J., 1975. The Mathematics of Diffusion, 2nd ed. Clarendon Press, Oxford.

Cvetkovic, V., Painter, S., Outters, N., Selroos, J., 2004. Stochastic simulation of radionuclide migration in discretely fractured rock near the aspo hard rock laboratory. Water Resources Research 40, W02404. (PT: J; NR: 50; TC: 37; J9: WATER RESOUR RES; PG: 16; GA: 775RG).

Davy, P., Bour, O., Dreuzy, J.R.D., Darcel, C., 2006. Flow in multiscale fractal fracture networks. Geological Society, London, Special Publications 261, 31–45.

Davy, P., Goc, R.L., Darcel, C., 2010. A likely universal model of fracture scaling and its consequence for crustal hydromechanics rid b-1417-2012. Journal of Geophysical Research—Solid Earth 115, B10411. (PT: J; NR: 81; TC: 2; J9: J GEOPHYS RES-SOL EA; PG: 13; GA: 666EK).

Dershowitz, W., Miller, I., 1995. Dual-porosity fracture flow and transport. Geophysical Research Letters 22, 1441–1444. (PT: J; NR: 22; TC: 22; J9: GEOPHYS RES LETT; PG: 4; GA: RB550).

Doughty, C., Karasaki, K., 2002. Flow and transport in hierarchically fractured rock. Journal of Hydrology 263, 1–22. (PT: J; TC: 16).

de Dreuzy, J.R., Davy, P., 2007. Relation between fractional flow models and fractal or long-range 2-d permeability fields. Water Resources Research 43, W04431. (PT: J; TC: 3; UT: WOS:000246147500006).

de Dreuzy, J.R., Davy, P., Bour, O., 2001. Hydraulic properties of two-dimensional random fracture networks following a power law length distribution 1. Effective connectivity. Water Resources Research 37, 2065–2078. (PT: J; TC: 49; UT: WOS:000170090100004).

Haggerty, R., Gorelick, S.M., 1995. Multiple-rate mass-transfer for modeling diffusion and surface-reactions in media with pore-scale heterogeneity. Water Resources Research 31, 2383–2400. (PT: J; TC: 252).

Haggerty, R., McKenna, S.A., Meigs, L.C., 2000. On the late-time behavior of tracer test breakthrough curves. Water Resources Research 36, 3467–3479. (PT: J; TC: 128; UT: WOS:000165799100006).

Hamm, S.Y., Bidaux, P., 1996. Dual-porosity fractal models for transient flow analysis in fissured rocks. Water Resources Research 32, 2733–2745. (PT: J; TC: 23; UT: WOS:A1996VE90100009).

Hassanzadeh, H., Pooladi-Darvish, M., 2006. Effects of fracture boundary conditions on matrix-fracture transfer shape factor. Transport in Porous Media 64, 51–71. (PT: J; TC: 6; UT: WOS:000237826900004).

Hassanzadeh, H., Pooladi-Darvish, M., Atabay, S., 2009. Shape factor in the draw-down solution for well testing of dual-porosity systems. Advances in Water Resources 32, 1652–1663. (PT: J; TC: 1).

Lagendijk, V.R., Vogel, T., Kongeter, J., Jansen, D., 2000. Contaminant transport modeling in multi-porosity fractured systems using a multi-continuum approach. Geoecology and Computers, 497–502.

Lim, K.T., Aziz, K., 1995. Matrix-fracture transfer shape factors for dual-porosity simulators. Journal of Petroleum Science and Engineering 13, 169–178. (PT: J; TC: 29).

Liu, H., Bodvarsson, G., Pan, L., 2000. Determination of particle transfer in random walk particle methods for fractured porous media. Water Resources Research 36, 707–713. (PT: J; NR: 18; TC: 19; J9: WATER RESOUR RES; PG: 7; GA: 287RL).

Maloszewski, P., Zuber, A., 1993. Tracer experiments in fractured rocks—matrix diffusion and the validity of models. Water Resources Research 29, 2723–2735. (PT: J; TC: 95; UT: WOS:A1993LR88400021).

Neretnieks, I., 1980. Diffusion in the rock matrix—an important factor in radio-nuclide retardation. Journal of Geophysical Research 85, 4379–4397. (PT: J; TC: 377).

Neuman, S.P., 2005. Trends, prospects and challenges in quantifying flow and transport through fractured rocks. Hydrogeology Journal 13, 124–147. (PT: J; TC: 105).

Painter, S., Cvetkovic, V., 2005. Upscaling discrete fracture network simulations: an alternative to continuum transport models. Water Resources Research 41, W02002. (PT: J; NR: 41; TC: 19; J9: WATER RESOUR RES; PG: 10; GA: 895ZQ).

Roubinet, D., de Dreuzy, J.R., Tartakovsky, D.M., 2012. Semi-analytical solutions for solute transport and exchange in fractured porous media. Water Resources Research 48, W01542. (PT: J; TC: 0; UT: WOS:000299702600003).

Roubinet, D., Liu, H.H., de Dreuzy, J.R., 2010. A new particle-tracking approach to simulating transport in heterogeneous fractured porous media. Water Resources Research 46, W11507. (PT: J; TC: 0).

Sahimi, M., 1993. Flow phenomena in rocks—from continuum models to fractals, percolation, cellular-automata, and simulated annealing. Reviews of Modern Physics 65, 1393–1534. (PT: J; TC: 506; UT: WOS:A1993MM65700007).

Shan, C., Pruess, K., 2005. An analytical solution for slug tracer tests in fractured reservoirs. Water Resources Research 41, W08502. (PT: J; TC: 1; UT: WOS:000231384800006).

Sudicky, E.A., Frind, E.O., 1982. Contaminant transport in fractured porous-media—analytical solutions for a system of parallel fractures. Water Resources Research 18, 1634–1642. (PT: J; TC: 276).

Tang, D.H., Frind, E.O., Sudicky, E.A., 1981. Contaminant transport in fractured porous-media—analytical solution for a single fracture. Water Resources Research 17, 555–564. (PT: J; TC: 317).

Warren, J.E., Root, P.J., 1963. The behavior of naturally fractured reservoirs. Society of Petroleum Engineers Journal 3, 245–255. (PT: J; TC: 410).

Zhou, Q., Liu, H.H., Molz, F.J., Zhang, Y., Bodvarsson, G.S., 2007. Field-scale effective matrix diffusion coefficient for fractured rock: results from literature survey. Journal of Contaminant Hydrology 93, 161–187. (PT: J; TC: 18).